Proceedings of ICRC 2001: 1671 © Copernicus Gesellschaft 2001

ICRC 2001

Isotopic measurements of cosmic-ray hydrogen and helium during the 1997 solar minimum

J. Z. Wang[1], E.S. Seo[1], R. W. Alford[1], K. Abe[2], K. Anraku[2], K. Asaoka[2], M. Fujikawa[2], M. Imori[2], T. Maeno[2], Y. Makida[3], N. Matsui[2], H. Matsumoto[4], H. Matsunaga[2, †], J. Mitchell[5], T. Mitsui[4, ‡], A. Moiseev[5], M. Motoki[2, ‡], J. Nishimura[6], M. Nozaki[4], S. Orito[2, *], J. Ormes[5], T. Saeki[2], T. Sanuki[2], M. Sasaki[4], Y. Shikaze[2], T. Sonoda[2], R. Streitmatter[5], J. Suzuki[3], K. Tanaka[3], I. Ueda[2], Y. Yajima[6], T. Yamagami[6], A. Yamamoto[3], T. Yoshida[3], and K. Yoshimura[2]

[1]IPST, University of Maryland, College Park, MD 20742, USA
[2]University of Tokyo, Tokyo 113-0033, JAPAN
[3]KEK, Tsukuba, Ibaraki, 305-0801, JAPAN
[4]Kobe University, Kobe, Hyogo 657-8501, JAPAN
[5]NASA GSFC, Code 660, Greenbelt, MD20771, USA
[6]ISAS, Sagamihara, Kanagawa 229-8510, JAPAN

Abstract. The balloon-borne BESS experiment was successfully flown from Lynn Lake, Canada during the most recent solar minimum on July 27, 1997. The instrument was reconfigured with a new Aerogel Cherenkov counter for this flight. The time-of-flight system was greatly improved, and achieved excellent time resolution of 50 picoseconds. Isotopes of cosmic-ray hydrogen and helium were well separated with rigidity up to 6 GV. This is the first composition measurement with rigidity up to 6 GV during a solar minimum. The precise measurement of hydrogen and helium energy spectra and their isotopic composition are presented in this paper.

1 Introduction

Accurate measurement of the energy spectra and isotopic composition of hydrogen and helium can provide information on the cosmic-ray origin and propagation history in interstellar space. The absolute fluxes at solar minimum provide the closest approximation to those in the local interstellar medium outside the heliosphere. The relative abundance of hydrogen and helium isotopes, with different rigidities at constant velocity, can place significant constraints on the modulation process. The Balloon Borne Experiment with a Superconducting Solenoid Spectrometer (BESS), which was flown annually since 1993, has been used to measure the cosmic-ray hydrogen and helium isotopes. Among these successive flights, BESS 97 is the one at solar minimum, and thus with the least solar modulation. In this paper, we present the energy spectra and the isotopic compositions measured during BESS 97.

The BESS spectrometer was designed and constructed as a high-resolution instrument (Orito, 1987; Yamamoto et al., 1994; Ajima et al., 2000) to conduct searches for antimatter in cosmic-rays, and to make precise measurements of various cosmic-ray components. The BESS 97 balloon flight was carried out on July 27, 1997, from Lynn Lake Canada. The instrument was reconfigured with a new Aerogel Cherenkov counter for this flight. The time-of-flight system was greatly improved, achieving excellent time resolution of 50 picoseconds for each counter, with a velocity $\beta(\beta \equiv V/c)$ resolution of 0.008. Figure 1 shows the continuous improvements of the TOF system for BESS 93, BESS 95 and BESS 97. Isotopes of cosmic-ray hydrogen and helium could be well separated with rigidity up to 6 GV in BESS 97. This is the first composition measurement with rigidity up to 6 GV during a solar minimum.

2 Data Analysis

2.1 Data selection

The unbiased count-down data were used in this analysis (see Seo et al. (1997, 2000); Wang et al. (2001)). Three kinds of event selection criteria were applied for both low threshold

Correspondence to: J. Z. Wang (jzwang@glue.umd.edu)
† Currently at Univ. of Tsukuba, Tsukuba, Ibaraki 305-8571, Japan
‡ Currently at Tohoku Univ., Sendai, Miyagi 980-8578, Japan
* deceased

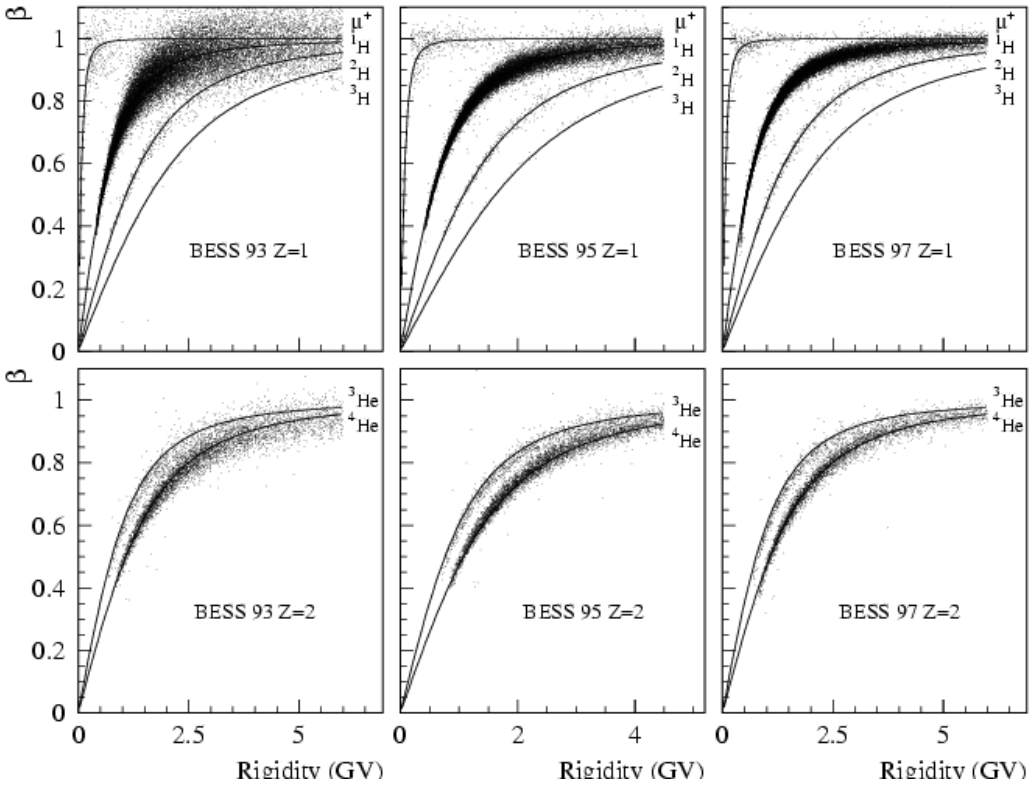

Fig. 1. Velocity measured from the time of flight versus rigidity for BESS 93, 95 and 97. The solid curves show the theoretical relation between velocity and rigidity for muons, protons, deuterons, tritium, ^{3}He and ^{4}He.

and high threshold data sets: (a) single-track cuts, (b) track quality cuts, and (c) consistency cuts (Wang et al., 2001). The charge one (Z = 1) and charge two (Z = 2) candidates were selected by the single-track cuts and the ionization energy loss (dE/dx) cuts. Events with nuclear interactions in the BESS instrument were removed by the single-track cuts. The efficiencies of the single-track cuts were calculated with Monte-Carlo simulations as described in the following subsection. The latter two cuts ((b) and (c)) were used to select events with high precision of the rigidity and velocity measurement. For Z = 1 and Z = 2 particles the efficiencies were 76% and 81% respectively. For the isotopic analysis, the mass of each particle was calculated from β and rigidity: $m^2_{TOF} = Z^2R^2(1/\beta^2 - 1)$. The mass histograms for each charge group, Z = 1 and Z = 2, are shown in Figures 2 and 3, respectively. The ^{2}H and ^{3}He are well separated from ^{1}H and ^{4}He, and they show good Gaussian fits up to 2 GeV/nucleon.

2.2 Simulations

Monte-Carlo simulations are essential for understanding instrument performance and acceptance (Wang et al., 2001). The most important requirement in determining the absolute fluxes is knowledge of the detector efficiencies (e.g. the effective geometry factors). We have performed full Monte-Carlo simulations of the BESS 97 configuration for both protons and heavy ions. Several simulation packages were combined in the simulation code developed for this study. GEANT was used for tracking and steering the simulation process, and the LaRC model was implemented to calculate the cross sections for nuclear interactions. While Fluka was used to simulate p + N interactions, RQMD and FRITIOF were used to simulate heavy ion interactions. A summary of the simulation details is described in Wang et al. 2001. The effective geometry factors at 1 GeV/nucleon are 0.23, 0.22, 0.19 and 0.19 m^{2}sr for ^{1}H, ^{2}H, ^{3}He and ^{4}He, respectively. There is an energy dependence of about 17% for protons at energies below 1 GeV/nucleon due to ionization and nuclear interactions, and about 32% for ^{4}He at higher energies up to above 100 GeV/nucleon due to delta ray effects.

2.3 Atmospheric corrections

The atmospheric corrections included two parts: (a) atmospheric attenuation and (b) secondary particle production. The attenuation loss was calculated with Monte-Carlo simulations. The particle loss fractions due to nuclear interactions in the 5 g/cm^2 atmospheric overburden were 6%, 8% 12% and 11% for ^{1}H, ^{2}H, ^{3}He and ^{4}He, respectively, with little energy dependence. These results are consistent with the fractions calculated by using the attenuation lengths of 90 g/cm^2, 75 g/cm^2, 40 g/cm^2 and 45 g/cm^2, respectively, for ^{1}H, ^{2}H, ^{3}He and ^{4}He (Papini et al., 1993a,b, 1996; Davis et al., 1995).

In balloon experiments secondary particles produced in the atmosphere are measured along with the primary cosmic-

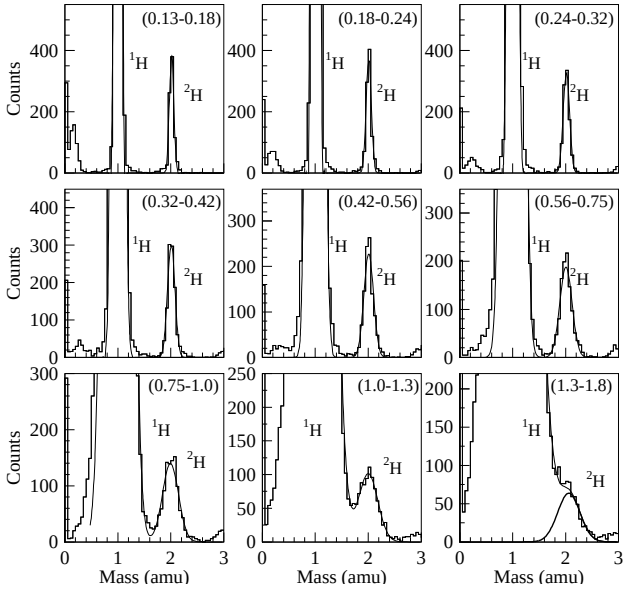

Fig. 2. Mass histograms of ^{2}H in energy bins corrected to top of atmosphere. The numbers shown in the figure are the energy bin range with the unit of GeV/nucleon. Because of their different energy loss rates, the ^{1}H shown along with the ^{2}H has higher energies than the ^{2}H in each bin.

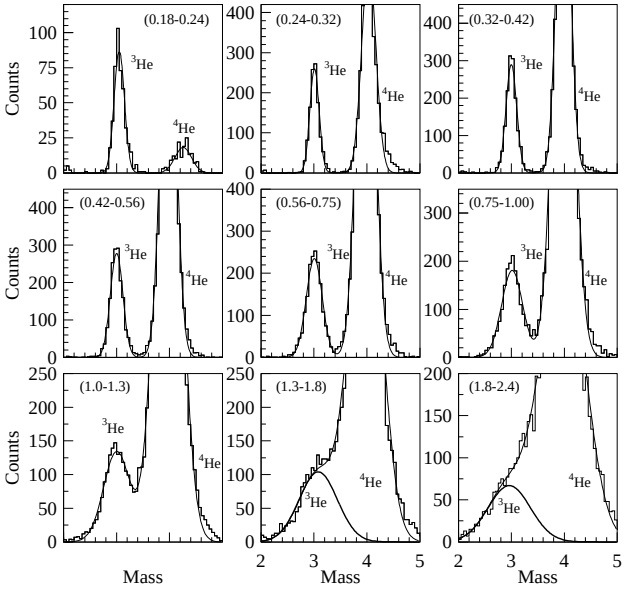

Fig. 3. Mass histograms of ^{3}He in energy bins corrected to top of atmosphere. The numbers shown in the figure are the energy bin range with the unit of GeV/nucleon. Because of their different energy loss rates, the ^{4}He shown along with the ^{3}He has higher energies than the ^{3}He in each bin.

rays. Secondary corrections become very important to get the cosmic-ray spectra at the top of the atmosphere, especially for Z = 1 particles at low energies. Secondary corrections for ^{2}H and ^{3}He are sensitive to the flux of primaries (proton and ^{4}He, etc.). The BESS 97 primary proton and ^{4}He spectra, measured simultaneously and reported in this paper, were used in this calculation.

2.4 Flux and Uncertainties

The count spectra N(E) of selected H and He isotopes were normalized to the final energy spectra. The differential fluxes at the top of the atmosphere as a function of kinetic energy per nucleon, E, are given by

$$F_{TOA}(E) = \left(\frac{N(E) C_d}{E_{gf}(E) E_c T \Delta E_{in}} - f_{sec}(E) \right) \frac{\Delta E_{in}}{\eta(E) \Delta E_{TOA}}, \quad (1)$$

where C_d is the inverse of the count-down rate, E_{gf}(E) is the energy-dependent effective geometry factor, E_c is the efficiency of the data selection cuts, T is the live time, ΔE_{in} is the bin size of kinetic energy at the BESS float altitude and corresponds to ΔE_{TOA} at the top of the atmosphere, η(E) is the correction factor for attenuation loss, and f_{sec}(E) is the atmospheric secondary spectra.

The uncertainties in the final spectra come from several sources: statistics, mass separation, effective geometry factors, atmospheric attenuation, and secondary production. Assuming these uncertainties are uncorrelated, we estimate that the uncertainties involved in our final spectra are 5%, 7%, 12% and 11% for hydrogen, helium and their isotopes, ^{2}H and ^{3}He, respectively, around 1 GeV/nucleon. The uncertainties are higher at both low and high energies. At low energy, the uncertainty comes mainly from the secondary correction. At high energy, it is due to statistical uncertainty and the greater difficulty in separating the isotopes from the primaries. Consequently the corresponding uncertainty becomes higher.

3 Results

The absolute fluxes of hydrogen, helium and their isotopes, ^{1}H, ^{2}He, ^{3}He and ^{4}He, obtained by analyzing the BESS 97 data are shown in Fig. 4. Only statistical uncertainties are included in the error bars. A successive evolution of fluxes along with the solar modulation are clearly shown in the energy spectra measured by BESS 97 and earlier BESS flights, BESS 93, 94, 95 (Seo et al., 1997, 2000; Wang et al., 1999, 2001). The curves are a theoretical prediction based on the reacceleration model with modulation parameters 500 MV (solid curves), 600 MV (dashed curves) and 700 MV (dotted curves) (Seo & Ptuskin, 1994). Our resulting spectra are consistent with both previous observations and theoretical calculations.

Acknowledgements. This work was supported in the USA by NASA grants NAG5-5255 and NAG5-5308, and in Japan by Grant-in-Aid for Scientific Research, Monbusho. We thank the National Scientific Balloon Facility for balloon flight support.

References

Ajima, Y., et al. 2000, Nucl. Instr. Methods Phys. Res., A443, 71
Beatty, J. J. 1986, ApJ, 311, 425

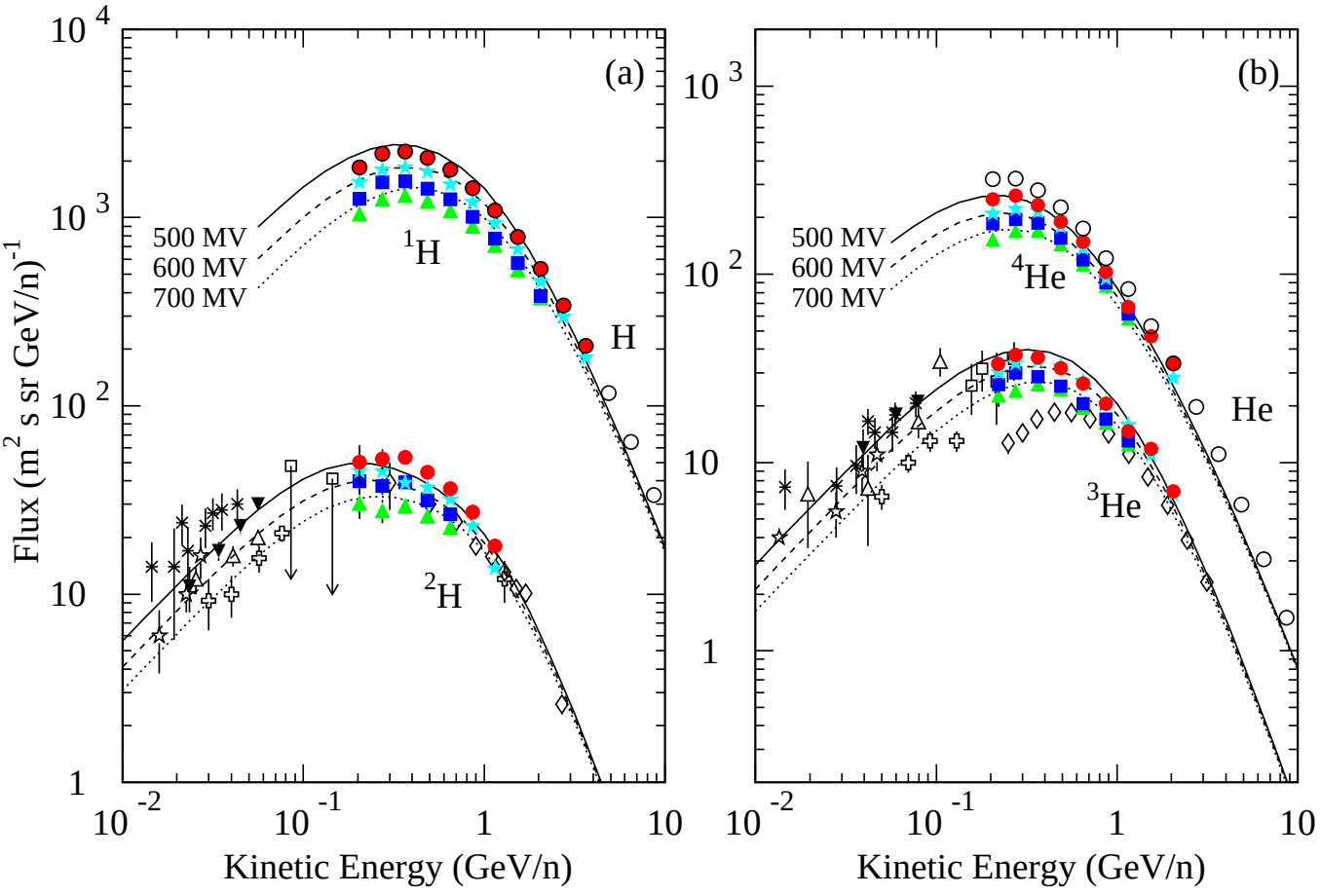

Fig. 4. BESS 97 differential energy spectra at the top of atmosphere for (a) hydrogen (open circles) and its isotopes, proton and deuteron (filled circles) (b) helium (open circles) and its isotopes, ^{3}He and ^{4}He (filled circles) , compared to other experimental data and theoretical calculations. The data points are as follows: open circles and filled circles, this work; filled stars BESS 95, filled squares, BESS 94, filled upward pointing triangles, BESS 93, Wang et al. (1999, 2001); open diamonds, Nolfo et al. (2000), Menn et al. (2000); open cross, Kroeger (1986), Bogomolov (1995); open squares, Leech & O'Gallagher (1978); filled downward pointing triangles, Beatty (1986); asterisks, Webber & Yushak (1983); open stars, Mewaldt et al. (1976); open upward pointing triangles, Garcia-Munoz et al. (1975a, 1975b). The curves represent calculated spectra using the reacceleration model with solar modulation parameters 500 MV (solid curves), 600 MV (dashed curves) and 700 MV (dotted curves).

Bogomolov, E. A., et al. 1995, Proc. 24th ICRC (Roma, 1995), 2, 598

Davis, A.J., et al. 1995, Proc. 24th ICRC(Rome), 2, 622

Garcia-Munoz, M., Mason, G.M., & Simpson, J.A. 1975a, Proc. 14th ICRC (Munich), 1, 319

Garcia-Munoz, M., Mason, G.M., & Simpson, J.A. 1975b, ApJ, 202, 265

Kroeger, R. 1986, ApJ, 303, 816

Leech, H. W., & O'Gallagher, J.J. 1978, ApJ, 221, 1110

Menn, W., et al. 2000, ApJ, 533, 281

Mewaldt, R. A., Stone, E. C., & Vogt, R. E. 1976, ApJ, 206, 616

Nolfo, G. A. de, et al. 2000, AIP Conf. Proc. 528, 425, ed. R. A. Mewaldt et al. (2000)

Orito, S. 1987, ASTROMAG Workshop, KEK Report 87-19, 111

Papini, P., Grimani, C., & Stephens, S.A. 1993a, Proc. 23rd ICRC (Calgary), 1, 499

Papini, P., Grimani, C., & Stephens, S.A. 1993b, Proc. 23rd ICRC (Calgary), 1, 503

Papini, P., Grimani, C., & Stephens, S.A. 1996, IL Nuovo Cimento, 19C, 367

Seo, E. S., & Ptuskin, V.S. 1994, ApJ, 431, 705

Seo, E. S., et al. 1997, Adv. Space Res., 19, 5, 751

Seo, E. S., et al. 1998, Adv. Space Res., 26, 11, 1831

Wang, J. Z., et al. 1999, Proc. 26th ICRC (Salt Lake City), 3, 37

Wang, J. Z., et al. 2001, ApJ, (submitted)

Webber, W. R., & Yushak, S.M. 1983, ApJ, 275, 391

Yamamoto, A., et al. 1994, Adv. Space Res., 14, 75